

Crystal Structure of the Explosive Parent Benzyne Precursor: 2-Diazoniobenzenecarboxylate Hydrate

Christopher J. Horan, Charles L. Barnes, and Rainer Glaser*

Department of Chemistry, University of Missouri-Columbia,
Columbia, Missouri 65211, USA

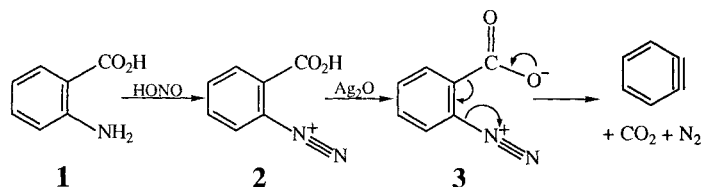
Received August 27, 1992

Key Words: Benzyne precursor / Neighboring group interactions / Incipient nucleophilic attack / 2-Diazoniobenzenecarboxylate / Calculations, ab initio, MO

The structure of the highly unstable benzyne precursor 2-diazoniobenzenecarboxylate (**3**) has been determined by single-crystal X-ray diffraction. The structure is discussed in comparison to ab initio results for several conformers of **3**, related aromatic diazonium ions, and phenyl cation and also to crystal

structures of simple diazonium ion salts and of benzoates. Structural features and characteristic distortions are related to the electron density distributions and to intra- and intermolecular interactions between the neighboring functional groups.

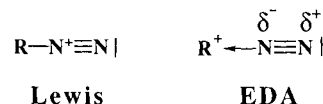
Of the numerous reactions that introduce or interchange substituents on aromatic rings, the "elimination-addition" mechanism involves the unstable intermediate benzyne. One of the most useful methods for the generation of benzyne is the diazotization of anthranilic acid^[1] to the zwitterion **3**, followed by loss of N₂ and CO₂.



Much spectroscopic work including ultraviolet, infrared, and mass spectra has previously been reported demonstrating the existence of benzyne^[2,3]. Most recently, Radziszewski et al. have carried out both infrared studies and extensive ab initio studies on benzyne, and they have assigned a band at 1846 cm⁻¹ to the triple bond stretch of benzyne^[4]. Mechanistic studies have shown that the decomposition of **3** actually involves benzyne as an intermediate. The formation of dibenzocyclobutadiene indicates dimerization of the intermediate benzyne^[2], and benzyne has been trapped with various 4π-electron systems as the products of [4 + 2] cycloaddition reactions^[5].

We have now successfully determined the crystal structure of the explosive precursor of benzyne. This crystal structure was determined as part of our studies of the "incipient nucleophilic attack" in diazonium ions to probe for their electronic structures. We have recently proposed a new bonding model for diazonium ions based on topological electron density analysis (EDA)^[6]. In contrast to the Lewis structure which implies that the N₂ function carries the positive charge, in our bonding model diazonium ions are best described as carbenium ions associated with an N₂ group that is internally polarized in the fashion Nα^{δ-}—Nβ^{δ+}. We tested the ability of our new bonding model to explain the distortions in isomers of 3-diazoniumpropenoic acid, and the results fully support the new model^[7]. Since all of the

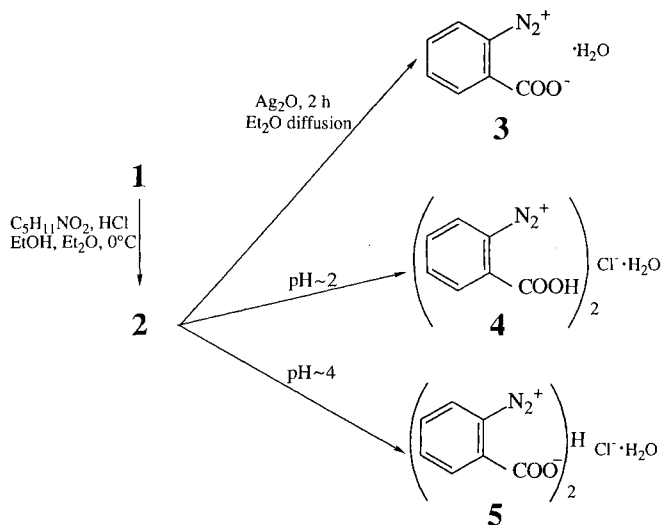
diazonium ions that we studied have rather common features, it seems reasonable to assume that our findings would carry over to larger systems for which experimental data exists. Distortions that occur in the crystal structure **3** which are caused by the intra- and intermolecular neighboring group interactions between the N₂ group and the *ortho*-COO⁻ group can serve to further test our new bonding model.



Crystal and Ab Initio Structures

Anthranilic acid (**1**) was diazotized with isoamyl nitrite and HCl to afford the intermediate diazonium chloride salt **2** (Scheme 1). At pH ≈ 2, we were able to crystallize the

Scheme 1



hydrate of the fully protonated acid **4**. Crystallization of **2** at pH \approx 4 resulted in partial deprotonation and crystals of the H-bridged dimer **5** were obtained. Complete deprotonation of **2** with wet Ag₂O yielded the highly unstable 2-diazoniobenzenecarboxylate zwitterion **3**. We have recently reported the crystal structures of **4** and **5** elsewhere^[8].

A perspective ORTEP II drawing^[9] of the crystal structure of **3** with the numbering scheme is shown in Figure 1, a stereoview molecular packing diagram is depicted in Figure 2, and final positional parameters are listed in Table 1.

For the isolated zwitterion **3**, we first performed geometry optimizations at the restricted Hartree-Fock (RHF) level with the 3-21G basis set within C_s symmetry^[10]. The Hessian matrix was then calculated analytically at this level to determine whether the planar structure was a minimum. Indeed, the vibrational frequencies calculated for **3** all were found to be positive. The structure of **3** was subsequently refined by optimization with the 6-31G* basis set. Structural parameters obtained at both theoretical levels are shown in Figure 3.

The agreement between the ab initio structures and our X-ray determination is generally very good. All characteristic structural features of **3** are manifested in the calculated

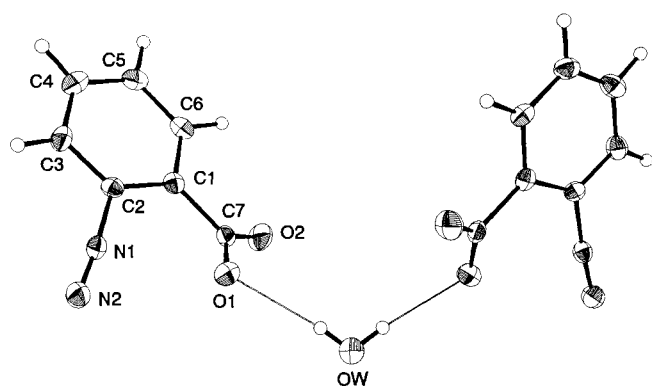


Figure 1. Perspective view of the zwitterionic **3** with numbering scheme. Thermal ellipsoids are drawn at the 50% probability level. Selected important bond lengths (in Å) include C(1)–C(2) = 1.398(2), C(1)–C(7) = 1.526(3), C(7)–O(1) = 1.250(3), C(7)–O(2) = 1.239(2), C(2)–N(1) = 1.406(4), N(1)–N(2) = 1.090(3), and important bond angles (in degrees) include C(1)–C(7)–O(1) = 115.9(2), C(1)–C(7)–O(2) = 115.8(2), O(1)–C(7)–O(2) = 128.3(2), C(2)–C(1)–C(7) = 122.3(2), C(1)–C(2)–N(1) = 118.5(2), C(2)–N(1)–N(2) = 174.3(2).

Table 1. Positional and equivalent isotropic thermal parameters^[20], with e.s.d.'s in parentheses

Atom	x	y	z	B _{iso} ^[a]
C(1)	0.2731(1)	0.2483(2)	0.3330(2)	1.50(6)
C(2)	0.1724(1)	0.2680(2)	0.3454(2)	1.51(5)
C(3)	0.1027(1)	0.2334(2)	0.2747(2)	1.92(7)
C(4)	0.1354(1)	0.1751(2)	0.1850(2)	2.15(6)
C(5)	0.2345(1)	0.1490(2)	0.1693(2)	1.97(7)
C(6)	0.3018(1)	0.1850(2)	0.2420(2)	1.76(6)
C(7)	0.3456(1)	0.2950(2)	0.4136(2)	1.63(6)
O(1)	0.31780(8)	0.4126(2)	0.4747(1)	2.16(4)
O(2)	0.4247(1)	0.2118(2)	0.40977	2.71(5)
N(1)	0.13692(9)	0.3186(2)	0.4377(2)	1.62(6)
N(2)	0.10236(9)	0.3523(2)	0.5069(2)	2.31(6)
O(W)	1/2	1/2	0.5903(2)	3.26(8)

^[a] B_{iso} is the mean of the principal axes of the thermal ellipsoid.

structures as well. For the benzene ring, the largest bond deviation between our experimental and theoretical values is 0.016 Å for the C(2)–C(1) bond, and the largest angle deviation found is 0.48° for the C(2)–C(1)–C(6) angle. The structural parameters of the diazo function agree equally well but more significant differences between the X-ray structure and theory do occur for the carboxylate group and they can be understood considering the relative arrangements of the zwitterions in the crystal (vide infra).

For the discussion of the ring deformations, the structure of phenyl cation will be relevant and since its structure has not been determined experimentally we take recourse to ab initio theory^[11]. In Figure 3, the structural parameters of phenyl cation are given that are obtained at the levels RHF/6-31G* and at the correlated level MP2(full)/6-31G*. Vibrational frequency calculation at the RHF/6-31G* level indicates that C_{2v} symmetric phenyl cation is a minimum. In the following, we will refer to the higher level result unless otherwise noted.

Structural Characteristics of the Zwitterion **3**

Benzene Ring Deformation: The angles and bond lengths in the phenyl ring of **3** are distorted qualitatively in the same way as those found in phenyl cation and in other benzenediazonium salts PhN₂⁺ X[−] with X[−] = Cl[−], Br₃[−],

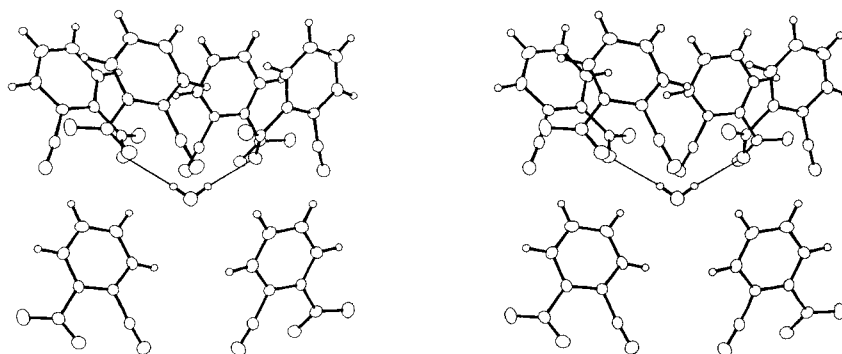


Figure 2. Stereoview of the packing interactions

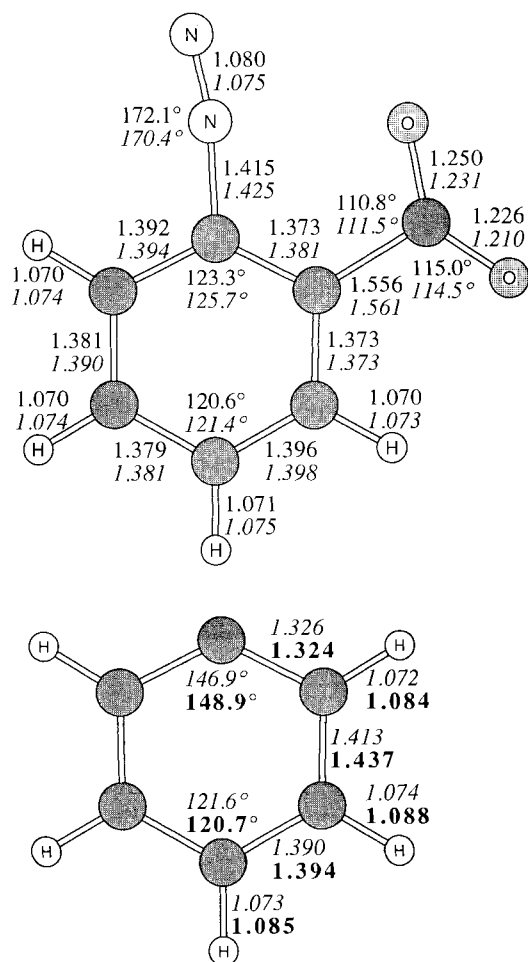


Figure 3. Molecular model of the ab initio optimized C_s structure of **3** and the C_{2v} structure of phenyl cation. Structural parameters are those derived at the theoretical levels RHF/3-21G, RHF/6-31G* (in italics), and at MP2(full)/6-31G* (in bold)

BF_4^- ^[12]. To describe the benzene ring distortions, it is convenient to use the parameters Θ , a , b , c and their differences u , v , w as defined in Table 2. Note that these parameters are defined without recourse to symmetry elements and they can therefore be used in discussions of the C_{2v} -type deformations in the simple salts $PhN_2^+X^-$ as well as for the description of the same type of effect in molecules of lower symmetry. Also listed in Table 2 are the calculated parameters of **3**. As can be seen, there are only small differences between the calculated and the experimental bond lengths and bond angles indicating that solid-state effects on these "hard" parameters are essentially negligible. Note that the agreement between the RHF/6-31G* derived values and the X-ray data is excellent. In the calculation with the unpolarized basis set, the Θ angle is underestimated and consequently the RHF/3-21G data differ primarily in the a value and the parameters derived with it.

In phenyl cation, the $C(1)-C(2)-C(3)$ angle at the electron-deficient carbon is greatly increased to about 149° in order for the C^+ to increase its s character. As listed in Table 2, the $C(1)-C(3)$ distance in these salts increases ($a = 2.413-2.492$ Å) as the angle at $C(2)$ increases ($\Theta =$

$124.9^\circ-131.3^\circ$) distorting the phenyl ring from D_{6h} symmetry. The characteristic distortions of the benzene ring in **3** are caused primarily by the diazonium substituent, with only modest additional effects by the carboxylate group. In Figure 4, the values u , v and w are plotted versus the Θ angles and the correlations are well described by simple linear regression^[13]. We find $a > b$ and $u > 0$ in all cases. Except for the phenyl cation, the cationic systems all have c values that are larger than the a and b values.

Because of $u > 0$ the relation $v > w$ also holds. Note that the plots indicate essentially $u = 0$ for $\Theta = 120^\circ$ while

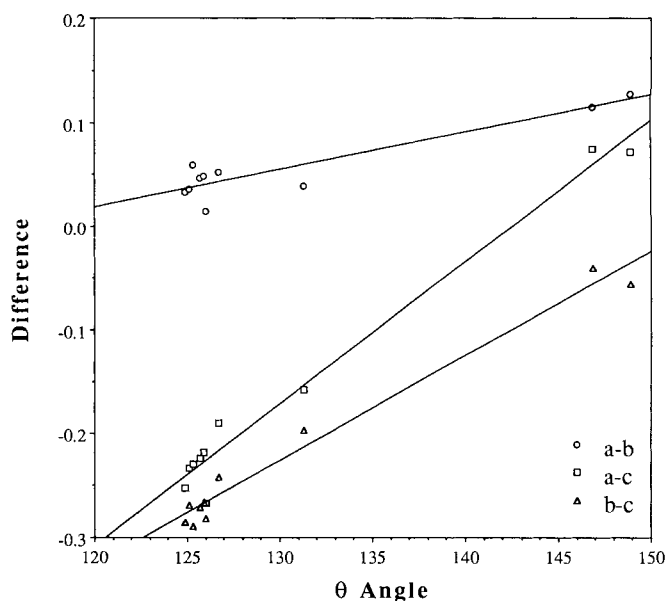


Figure 4. Deformation of benzene in benzenediazonium ions and related systems

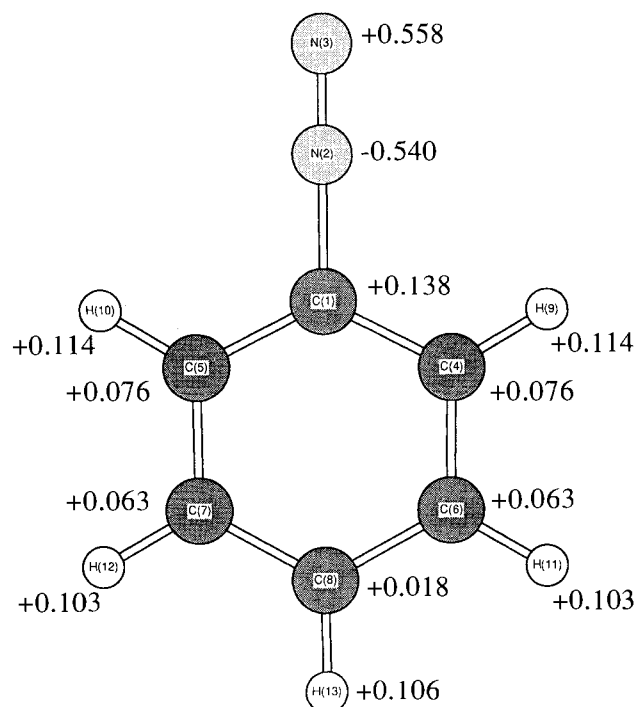


Figure 5. Integrated atomic charges of benzenediazonium ion at RHF/6-31G* level

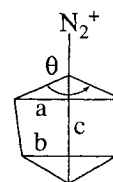


Table 2. Distortions in benzenediazonium ions and phenyl cation

Molecule ^[b]	a ^[a]	b	c	θ	u=a-b	v=a-c	w=b-c
Benzene, X-ray ^[21]	2.421	2.421	2.421	120.0	0.000	0.000	0.000
3 , X-ray	2.473	2.414	2.703	125.3	0.059	-0.230	-0.289
3 , RHF/3-21G	2.433	2.411	2.720	123.3	0.022	-0.287	-0.309
3 , RHF/6-31G*	2.470	2.423	2.694	125.7	0.047	-0.224	-0.271
Restricted, RHF/3-21G	2.441	2.413	2.716	123.6	0.028	-0.275	-0.303
Restricted, RHF/6-31G*	2.473	2.425	2.691	125.9	0.048	-0.218	-0.266
TS, RHF/3-21G	2.466	2.426	2.696	125.1	0.040	-0.230	-0.270
TS, RHF/6-31G*	2.488	2.436	2.678	126.7	0.052	-0.190	-0.242
PhN ₂ ⁺ Cl ⁻	2.436	2.403	2.689	124.9	0.033	-0.253	-0.286
PhN ₂ ⁺ Br ₃ ⁻	2.492	2.453	2.650	131.3	0.039	-0.158	-0.197
PhN ₂ ⁺ BF ₄ ⁻	2.413	2.398	2.680	126.0	0.015	-0.267	-0.282
PhN ₂ ⁺ , RHF/3-21G	2.447	2.419	2.716	123.6	0.028	-0.269	-0.297
PhN ₂ ⁺ , RHF/6-31G*	2.468	2.432	2.701	125.1	0.036	-0.233	-0.269
Ph ⁺ , RHF/6-31G*	2.542	2.427	2.467	146.9	0.115	0.075	-0.040
Ph ⁺ , MP2(full)/6-31G*	2.551	2.423	2.479	148.9	0.128	0.072	-0.056

^[a] Distances *a*, *b*, and *c* in Å and angles Θ in degrees. — ^[b] X-ray crystal structure data unless the theoretical model is specified.

the corresponding *v* and *w* values are -0.308 and -0.327 , respectively. These very substantial deviations from the corresponding values in the unperturbed benzene ($v = w = 0$) provide compelling structural evidence showing that the phenyl groups in Ph-H and Ph-N₂⁺ are rather distinct. These structural differences are just another reflection of the actual charge distribution in diazonium ions R-N₂⁺, namely, that the positive charge is not located on the N₂ but on the R group. We have shown this before for a variety of aliphatic diazonium ions^[6,7], but it is also true for the phenyl diazonium^[14] ion (Figure 5), and preliminary results suggest that this result even carries over to more highly substituted phenyldiazonium ions.

Carboxylate Group Deformations: The C(1)–C(7) distance in **3** is 1.526(3) Å and significantly longer than the bond length of 1.46 Å or a standard C–C single bond between sp²-hybridized carbons^[15]. The respective bond lengths in other benzoates fall in the range of 1.49 Å to 1.64 Å^[16]. Thus, the CO₂ group seems to be involved in little to no conjugation with the phenyl ring. Another feature displaying this lack of conjugation is the substantial magnitude of the carboxylate group's rotation. In the solid-state structure of **3**, the carboxylate group is rotated by 25.9° out of the plane, indicating that the rotational barrier about the C–CO₂ bond can easily be overcome by intermolecular forces (vide infra).

We have investigated the energetics of the carboxyl rotation by considering the transition-state structure for carboxyl rotation in **3**, the rotational barrier in the *para* isomer

of **3**, the rotational barrier in the benzoate ion, and the energy requirements to twist the carboxyl group by the amount found in the crystal structure. All stationary structures were optimized in C_s symmetry at RHF/3-21G and RHF/6-31G* and confirmed to be minima or transition-state structures by computation of the vibrational frequencies at the lower level^[14]. The structure of **3** with the twisted carboxyl group was fully optimized with the one constraint on the torsion angle. We note that the bond lengths and angles in the resulting RHF/6-31G* structure are essentially unchanged compared to the planar structure of **3** with one important exception. The C–N–N angle is increased as expected and its value of 172.8° is even closer to the respective value found in the solid state. We report rotational barriers that include the scaled (factor 0.9) vibrational zero-point energy corrections. The rotational barrier of 7.02 kcal/mol in benzoate may serve as a reference. The rotational barrier in the *para*-diazoniobenzenecarboxylate is 4.68 kcal/mol. As expected, electron depletion of the phenyl ring caused by the *para*-diazonium function decreases the barrier for carboxyl rotation because it reduces π -electron donation from the phenyl ring toward the CO₂ carbon. In marked contrast, the *ortho* isomer **3** shows a larger rotational barrier of 9.90 kcal/mol. These rotational barriers of the isomeric structures clearly indicate attractive interactions between the substituents in the *ortho* isomer. The difference in these rotational barriers of 5.22 kcal/mol is a measure for the increased neighboring group interaction in **3** compared to its rotational transition state. Importantly, we find that for

small to moderate rotations around the C—CO₂ bond comparatively little energy is required. In particular, the distorted structure of **3** with the 25.9° torsion angle is only 1.50 kcal/mol less stable compared to planar **3**.

The CO₂ group in **3** exhibits a wide O(1)—C(7)—O(2) angle of 128.3° as is typical for benzoates^[16] in general. The calculated structures of **3** also show this angle widened but there is an interesting qualitative difference between the theoretical and the solid-state structures with regard to the C(1)—C(7)—O(1) and C(1)—C(7)—O(2) angles of the CO₂ group. In the planar calculated structure (Figure 3), these angles differ greatly and result in a tilt of the CO₂ group toward the N₂. We will provide an explanation for these differences below after our analysis of the intramolecular neighboring group interactions.

Intramolecular Neighboring Group Interaction

In **3**, the terminal nitrogen N(2) is displaced away from the carboxyl group resulting in a 5.7° deviation of the C(2)—N(1)—N(2) skeleton from linearity. This bending is consistent either with attraction of the proximate carbonyl oxygen atom (O_{pr}) and a positively charged N(1) (as suggested by the commonly used Lewis structure) or with quadrupolar neighboring interactions between N(1)^{δ-}—N(2)^{δ+} and the polar carbonyl group as suggested by our recently proposed bonding model^[6,7]. Our interpretation views the close approach of the proximate nucleophile (O_{pr}) to N(1) as a consequence of optimizing the attractive interactions between O_{pr} and the positive termini of the C(2)—N(1)≡N(2) fragment and this approach occurs despite N(1)—O_{pr} repulsion. The invocation of N(1)—O_{pr} repulsion is not only

consistent with but also provides a simple explanation for the observation that the N₂ and COO⁻ groups are on opposite sides of the best plane of the phenyl ring [dihedral angle N(1)—C(2)—C(1)—C(7): 5.1(1)°]. This displacement increases the N(1)—O_{pr} distance and thus seems inconsistent with the assumption of N(1)—O_{pr} attraction.

In a very closely related case, the structure of 3-carboxy-2-naphthalenediazonium chloride^[17], the two functional groups are on opposite sides of the naphthalene plane and the CNN skeleton also deviates from linearity in the discussed fashion, but these structural characteristics were interpreted with the N(1)—O_{pr} attraction model.

A significant difference occurs between our benzene derivative and the naphthalene derivative which has important consequences for the discussion of neighboring group interactions. In the crystal structure of 3-carboxy-2-naphthalenediazonium chloride, the carboxylate group is rotated only slightly out of the plane of the ring. Importantly, in the benzyne precursor **3**, the carboxylate group is rotated substantially around the C—CO₂ axis [C(2)—C(1)—C(7)—O(1): 25.9(1)°] in such a fashion that the N(1)—O_{pr} distance is increased. The rotation of the CO₂ group might be taken as a further manifestation of N(1)—O_{pr} repulsion but it might also be a consequence of the intermolecular interactions of the carboxylate groups with a neighboring C(2)—N(1)—N(2) fragment or with hydrogen bonding of the carboxylate groups with water found in the crystal lattice. Our theoretical study of the zwitterion **3** shows that the planar structure is the minimum for the free molecule and, hence, that the latter arguments are more important. We note again that only a comparatively small amount of energy is required to appropriately distort the planar structure (*vide supra*).

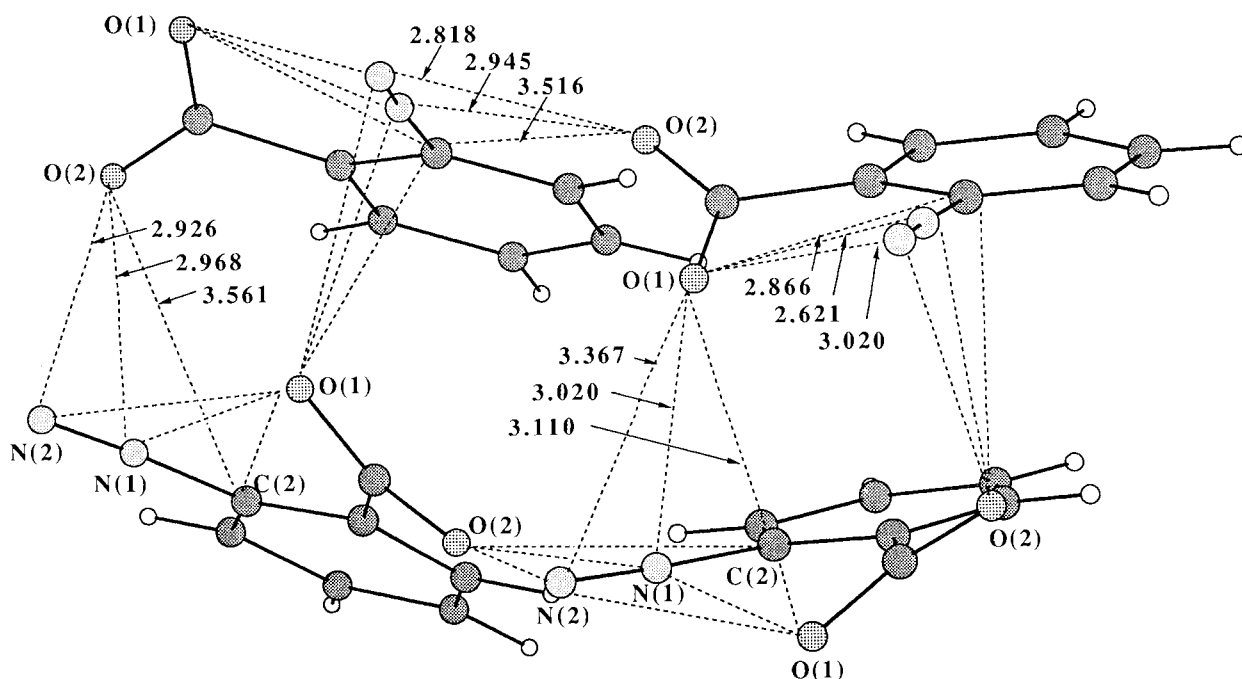


Figure 6. Edge-on view showing the intermolecular neighboring interactions between the carboxylate group of one zwitterion with the diazonium function of another. The water molecule has been excluded from this figure for clarity

In light of this analysis, it appears reasonable that the significant difference between the C(1)–C(7)–O(1) and C(1)–C(7)–O(2) angles of the CO₂ group in the theoretical and X-ray values are related to the torsion about the C–CO₂ bond. The intramolecular neighboring interaction of the proximate oxygen O(1) with the diazonium function results in an overall attractive interaction that leads to a contraction of the C(1)–C(7)–O(1) angle. In the X-ray structure of **3**, both angles in the carboxylate group are essentially equivalent due to the 25.9° rotation and, thus, the effects of the intramolecular neighboring group interaction of O(1) with the diazonium function no longer persist.

Intermolecular Neighboring Group Interactions

In **3**, the diazonium function of one zwitterion is stabilized by intermolecular interactions with the negatively charged carboxylate oxygens of neighboring zwitterions as shown in Figure 6. Each carboxylate oxygen assumes a 1,3-bridging position with regard to the C–N≡N group. Our recent topological studies of the electronic structures of diazonium ions – which revealed charge distributions of the type C(2)⁺ – δ[–]N(1)–N(2)^{δ⁺} – are fully consistent with such 1,3-bridging^[7]. In Figure 6, sets of three lines from each CO₂ oxygen toward a diazonium function are used to indicate such 1,3-bridging interactions and in this way it becomes apparent that each O(2) atom is involved in two intermolecular bridging interactions, while each O(1) is involved in one *inter*- and one *intramolecular* 1,3-bridging interaction. Every diazonium group is surrounded by four essentially equidistant negatively charged oxygen atoms. Note that the same type of coordination also is observed in the crystals of benzenediazonium chloride, tribromide, and tetrafluoroborate^[12] and, moreover, the distances between the four respective gegenions and the atoms of each diazonium function agree closely for these salts and for **3**.

It appears that it is the optimization of these electrostatic intermolecular interactions that are responsible for the torsion about the C–CO₂ bond in the solid state. For the isolated zwitterion – as in the theoretical model – a planar configuration is advantageous in which intramolecular neighboring group stabilizations with one diazonium function occur. In the solid-state structure, however, in which each molecule is surrounded by others, it is more advantageous for the rotated carboxylate groups to assume a structure that maintains this intramolecular interaction but at the same time allows for optimization of the intermolecular neighboring interactions of three separate diazonium functions as well.

Acknowledgment is made to the Donors of the *Petroleum Research Fund*, administered by the *American Chemical Society*, and to the *MU Research Council* (92-RC-023-BR) for support of this research. We thank the *NSF National Center for Supercomputing Applications*, Champaign-Urbana, Illinois, for computer time. C. J. H. gratefully acknowledges support by both a *Dorothy Nightingale Fellowship* and an *ABC Laboratories Fellowship*. The X-ray diffractometer was partially funded by the *National Science Foundation* (CHE 90-11804).

Experimental

2-Diaziobenzoic Acid (2): Following the procedure by Stiles et al.^[2b], a solution of 2.74 g (0.20 mmol) of anthranilic acid (Aldrich) in 30 ml of absolute ethanol was cooled to 0°C and treated with 2 ml of concentrated hydrochloric acid. The solution was again allowed to cool to 0°C, and 5.0 ml (0.38 mmol) of cold isoamyl nitrite was then added dropwise over 7–8 min to the stirred solution. The color of the solution changed to deep orange as the nitrite was added and faded to a lighter orange near the completion of the reaction. Addition of approximately 30 ml of ether caused precipitation of the crude diazonium chloride salt **2**, which was suction-filtered, washed with ether, and used without further purification.

2-Diaziobenzenecarboxylate Hydrate (3): The salt **2** was transferred to a clean flask and dissolved in the least amount (5.0–7.0 ml) of cold water. 3.0 g (0.13 mmol) of powdered silver oxide (Ag₂O) was added to the solution and the slurry was stirred at 0°C for 2 h. The solid material was filtered off, and the clear solution was added to a 0°C mixture of 45 ml ether and 80 ml of absolute ethanol.

Single-Crystal Preparation: Under refrigeration, ether was allowed to diffuse into the system over a 1–1.5-day period forming pale yellow crystals on the walls of the flask near the surface of the solution. Extreme caution had to be exercised when preparing the crystals for mounting. On several occasions, light scraping of the dried crystals led to violent detonations. To alleviate this problem, the crystals were picked directly from the ether/alcohol solution on the tip of a quartz fiber and without drying immediately placed in a stream of N₂.

X-ray Structure Analysis of 3: C₇H₄N₂O₂ · H₂O, *M_r* = 157.13, orthorhombic, space group *Aba2*, *a* = 13.719(2), *b* = 7.170(1), *c* = 13.742(2) Å, *V* = 1351.7(3) Å³, *Z* = 8, *D_x* = 1.544 g cm^{–3}, λ(Mo *K_α*) = 0.71073 Å, μ = 1.1 cm^{–1}, *F*(000) = 648. The data were collected at a temperature of 173°K on a Enraf-Nonius CAD4 diffractometer. The crystals were pale yellow prisms, 0.15 × 0.40 × 0.40 mm; density not measured; 25 reflections with 10° ≤ Θ ≤ 12.5°, Mo *K_α*, used to refine cell dimensions; systematic absences: *hkl*, *k* + *l* = 2*n* + 1, *hk0*, *k* = 2*n* + 1, and successful refinement; no absorption correction applied; 2Θ_{max} = 0.0°; 0 ≤ *h* ≤ 16, 0 ≤ *k* ≤ 8, 0 ≤ *l* ≤ 16; three standard reflections measured after every 3600 s of X-ray exposure indicated less than 2% decay; 959 total reflections 922 unique, *R_i* = 0.011, 912 observed [*I* ≥ 2.5σ(*I*)]; structure solved by direct methods; refinement on *F*, function minimized during refinement was Σw(*F_o* – *F_c*)², with *w* = 1/[σ²(*F*) + 0.0015(*F*)²]; H atoms located in difference-map and refined with fixed isotropic thermal parameters; non-H atoms refined with anisotropic thermal parameters. The polarity of the structure was not clearly established, refinement of the *Eta* parameter with the reported configuration gave *Eta* = +3 ± 7. *R* = 0.023, *R_w* = 0.033, *S* = 1.09; (Δ/σ)_{max} = 1.3%, final difference-map max.: 0.13, min.: –0.16 eÅ^{–3}. Atomic scattering factors and anomalous-dispersion corrections from International Tables for X-ray Crystallography^[18], structure solution and all calculations performed with the program NRCVAX^[19].

Supplement Material contains a complete set of internal coordinates, structure factors, positional parameters, and anisotropic thermal parameters. This material is available on request from the authors. Further details of the crystal structure investigation are available on request from the Director of the Cambridge Crystallographic Data Centre, University Chemical Laboratory, Lensfield Road, GB-Cambridge CB2 1EW (UK), on quoting the full journal citation.

- [1] A. Hantzsch, W. B. Davidson, *Ber. Dtsch. Chem. Ges.* **1896**, 29, 1535.
- [2] [2a] R. S. Berry, G. N. Spokes, M. Stiles, *J. Am. Chem. Soc.* **1962**, 84, 3570–3577. — [2b] M. Stiles, R. G. Miller, U. Burckhardt, *J. Am. Chem. Soc.* **1963**, 85, 1792–1797. — [2c] R. S. Berry, J. Clardy, M. E. Schaefer, *J. Am. Chem. Soc.* **1964**, 86, 2738–2739. — [2d] M. E. Schaefer, R. S. Berry, *J. Am. Chem. Soc.* **1965**, 87, 4497–4501.
- [3] [3a] O. L. Chapman, C.-C. Chang, J. Kolc, N. R. Rosenquist, H. Tomioka, *J. Am. Chem. Soc.* **1975**, 97, 6586–6588. — [3b] J. W. Laing, R. S. Berry, *J. Am. Chem. Soc.* **1976**, 98, 660–664. — [3c] C. Wentrup, R. Blanch, H. Briehl, G. Gross, *J. Am. Chem. Soc.* **1988**, 110, 1874–1880. — [3d] D. G. Leopold, A. E. S. Miller, W. C. Lineberger, *J. Am. Chem. Soc.* **1986**, 108, 1379–1384. — [3e] A. C. Scheiner, H. F. Schaefer, III, B. Liu, *J. Am. Chem. Soc.* **1989**, 111, 3118. — [3f] J. G. G. Simon, N. Muenzel, A. Schweig, *Chem. Phys. Lett.* **1990**, 170, 187.
- [4] J. G. Radziszewski, B. A. Hess, R. Zahradnik, *J. Am. Chem. Soc.* **1992**, 114, 52–57.
- [5] W. T. Ford, *J. Org. Chem.* **1971**, 36, 3979–3987.
- [6] [6a] R. Glaser, *J. Phys. Chem.* **1989**, 93, 7993–8003. — [6b] R. Glaser, *J. Comput. Chem.* **1990**, 11, 663–679. — [6c] R. Glaser, G. S.-C. Choy, M. K. Hall, *J. Am. Chem. Soc.* **1991**, 113, 1109–1120. — [6d] R. Glaser, G. S.-C. Choy, C. J. Horan, *J. Org. Chem.* **1992**, 57, 995–999.
- [7] R. Glaser, C. J. Horan, E. Nelson, M. K. Hall, *J. Org. Chem.* **1992**, 57, 215–228.
- [8] [8a] C. J. Horan, C. L. Barnes, R. Glaser, *Acta Crystallogr., Sect. C*, in press. — [8b] C. J. Horan, P. E. Haney, C. L. Barnes, R. Glaser, *Acta Crystallogr., Sect. C*, submitted.
- [9] C. K. Johnson, ORTEP II, **1976**, Report ORNL-5138, Oak Ridge National Laboratory, Tennessee, USA.
- [10] [10a] W. J. Hehre, L. Radom, P. v. R. Schleyer, J. A. Pople, *Ab Initio Molecular Orbital Theory*, John Wiley & Sons, New York, **1986**. — [10b] Calculations were performed with *Gaussian90* (Gaussian, Inc., Pittsburgh, PA, **1990**) in part on Silicon Graphics Personal Iris Workstations, on the IBM 3090 mainframe of the MU Campus Computing Center, and on the IBM 6000 Systems at the NSF National Center for Supercomputing Applications at Champaign-Urbana.
- [11] For previous studies of phenyl cation, see for example: [11a] J. D. Dill, P. v. R. Schleyer, J. S. Binkley, R. Seeger, J. A. Pople, E. Haselbach, *J. Am. Chem. Soc.* **1976**, 98, 5428–5431. — [11b] J. D. Dill, P. v. R. Schleyer, J. A. Pople, *J. Am. Chem. Soc.* **1977**, 99, 1–8. — [11c] M. Tasaka, M. Ogata, H. Ichikawa, *J. Am. Chem. Soc.* **1981**, 103, 1885–1891. — [11d] K. Krogh-Jespersen, J. Chandrasekhar, P. v. R. Schleyer, *J. Org. Chem.* **1980**, 45, 1608–1614.
- [12] [12a] C. Rømming, *Acta Chem. Scand.* **1963**, 17, 1444–1454. — [12b] O. Andresen, C. Rømming, *Acta Chem. Scand.* **1962**, 16, 1882–1889. — [12c] M. Cygler, M. Przybylska, R. Eloffson, *Can. J. Chem.* **1982**, 60, 2852–2855.
- [13] The regressions lines shown in Figure 4 are as follows: $u = 3.5872 \cdot 10^{-3} \Theta - 0.41154$ with $R^2 = 0.850$, $v = 1.3660 \cdot 10^{-2} \Theta - 1.9476$ with $R^2 = 0.978$, and $w = 1.0073 \cdot 10^{-2} \Theta - 1.5360$ with $R^2 = 0.977$. Note that the RHF/3-21G data were not included in Figure 4.
- [14] Details of these calculations will be published in a forthcoming full paper.
- [15] M. J. S. Dewar, W. Thiel, *J. Am. Chem. Soc.* **1977**, 99, 4907.
- [16] [16a] $d(C-CO_2) = 1.508(9) \text{ \AA}$ in (benzoato-*O,O'*)bis(2-dimethylaminoethanol)copper(II) benzoate: U. Turpeinen, R. Hämäläinen, *Acta Crystallogr., Sect. C*, **1985**, 41, 1728–1730. — [16b] $d(C-CO_2) = 1.498(4) \text{ \AA}$ in 2,4-diamino-5-(3,4,5-trimethoxybenzyl)pyrimidinium benzoate: G. Giuseppetti, C. Tadini, *Acta Crystallogr., Sect. C*, **1984**, 40, 650–653. — [16c] $d(C-CO_2) = 1.532(6) \text{ \AA}$ in a complex of benzoic acid with 2,4-diamino-5-(3,4,5-trimethoxybenzyl)pyrimidinium benzoate: G. Giuseppetti, C. Tadini, *Acta Crystallogr., Sect. C*, **1988**, 44, 856–860. — [16d] $d(C-CO_2) = 1.49(1) \text{ \AA}$ in ammonium hydrogen bisbenzoate: I. A. Oxton, T. S. Cameron, O. Knop, A. W. McCulloch, *Can. J. Chem.* **1977**, 55, 3831–3837. — [16e] $d(C-CO_2) = 1.64(1) \text{ \AA}$ in tetra-*n*-butylammonium benzoate hydrate: M. Bonamico, G. A. Jeffrey, R. K. McMullan, *J. Chem. Phys.* **1962**, 37, 2219–2231.
- [17] [17a] J. Z. Gougoutas, *Cryst. Struct. Commun.* **1982**, 11, 1305 to 1310. — [17b] J. Z. Gougoutas, J. Johnson, *J. Am. Chem. Soc.* **1978**, 100, 5816–5820.
- [18] International Tables for X-ray Crystallography, vol. IV, Kynoch Press, **1974**, Birmingham (Present distributor D. Reidel, Dordrecht).
- [19] E. J. Gabe, Y. Le Page, J.-P. Charland, F. L. Lee, *J. Appl. Cryst.* **1989**, 22, 384.
- [20] W. C. Hamilton, *Acta Crystallogr.* **1959**, 12, 609–610.
- [21] Neutron diffraction study of benzene at -135°C gives $C-C = 1.398 \text{ \AA}$: G. E. Bacon, N. A. Curry, S. A. Wilson, *Proc. Roy. Soc. London, Ser. A* **1964**, 279, 98–110.

[339/92]